

INTERNATIONAL SOCIETY FOR SOIL MECHANICS AND GEOTECHNICAL ENGINEERING



This paper was downloaded from the Online Library of the International Society for Soil Mechanics and Geotechnical Engineering (ISSMGE). The library is available here:

<https://www.issmge.org/publications/online-library>

This is an open-access database that archives thousands of papers published under the Auspices of the ISSMGE and maintained by the Innovation and Development Committee of ISSMGE.

South Toulon tunnel: Analysis of an instrumented section

J.P. Janin, D. Dias & R. Kastner

Université de Lyon, INSA-Lyon, LGCIE, Villeurbanne, France

F. Emeriault

Grenoble INP, Laboratoire 3SR, CNRS UMR 5521, Grenoble, France

A. Guilloux & H. Lebissonais

TERRASOL, Montreuil, France

ABSTRACT: Large tunnels in soft rock or hard soil are now often constructed using full face excavation associated with ground reinforcement. Such works induce complex interactions between the soil, the reinforcements and existing structures, which are difficult to model precisely. In order to improve the understanding of ground response to this tunnelling method, and to collect precise data for validating numerical models, two comprehensive monitoring sections have been installed during the construction of the south Toulon tunnel (France). The monitoring results of the “Alexander I” section are analyzed in this paper and a first example of 2D numerical back analysis is presented.

1 INTRODUCTION

The south Toulon tunnel will connect motorways A50 and A57 (direction Marseille-Nice). It is an urban shallow tunnel (12 m of diameter), excavated through very difficult heterogeneous soils. The construction method associates full face excavation and ground reinforcement ahead of the tunnel face by pipe umbrellas and face bolting. This construction technique induces complex interactions between the ground, the umbrella pipes, the face bolts and the surrounding existing structures. In an urban site such as the town of Toulon, it is essential to adapt the construction sequences and the amount of reinforcement in order to avoid a failure and to control the settlements. In the Toulon tunnel, the surface and building deformations are measured, with high frequency, by automatic theodolites (Cyclops). Every 9 m there is a measure profile. All measurements are immediately stored in a database with real time access for all the actors. This represents an efficient tool permitting to continuously adapt the tunnelling process as described by Janin *et al* (2011). But at the design phase, it remains difficult to assess the effect of the different construction and reinforcement elements on the control of the ground movements and settlements. Therefore, in addition to these regular measures, two particular sections were studied in further details, with additional instruments, to improve the

understanding of ground response and to collect precise data for validating numerical models. The aim of this paper is to present the most important results obtained on one of the sections, followed by a first example of 2D numerical back analysis.

2 PRESENTATION OF THE ANALYZED SECTION

The section analysed in this paper is situated in garden “Alexandre I” in the west side of Toulon at chainage PM 882.

2.1 Instrumentation

The instruments set up from the surface in the section are (see Fig. 2.1):

- 2 inclinometers, 52 m deep, on both sides of the tunnel and 13 m from the axis;
- 1 vertical extensometer on the tunnel axis, 20 m long;
- 3 target prisms close to the previous instruments.

The instruments set up from the tunnel are:

- 4 radial extensometers, 13 m long;
- 6 vibrating strain gauges placed on the steel rib;
- 5 pressure cells;
- Convergence targets.

Table 2.1 shows the accuracy of each instrument and measures:

Table 2.1. Precision of instruments and measures:

Instrument/measures	Precision
Inclinometer	1 mm
Extensometer	0.5 mm
Theodolites—prism	0.5 mm
Radial extensometer	0.1 mm
Strain gauges	1 à 10 microstrains
Pressure cells	2 kPa
Tunnel convergence and settlements	2 mm

2.2 Geology

Based on the drilling information a geological profile has been proposed (see Fig. 2.1). It shows that the geological stratigraphy is generally horizontal and it highlights the high degree of alteration of the Basement. This alteration causes important variations of material characteristics.

The average ground properties of the different strata of the section, as retained for the detailed design, are presented in the table below:

Table 2.2. Hypothesis – geotechnical parameters Mohr-Coulomb.

Soils	γ (kN/m ³)	E (MPa)	c (kPa)	ϕ (°)	ψ (°)	ν
Colluviums	20.8	40	10	30	0	0.3
Basement	24.2	120	30	25	0	0.3

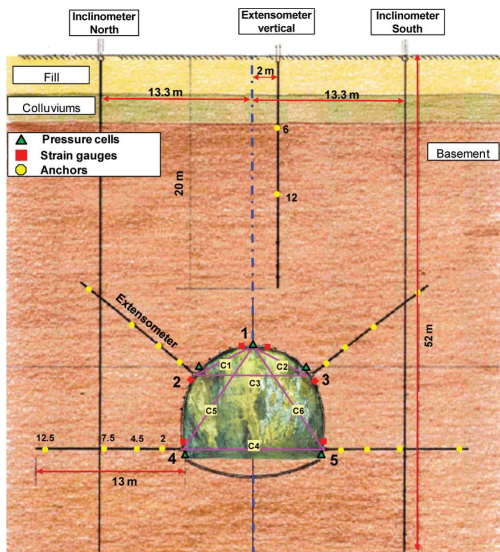


Figure 2.1. Geological section and instruments.

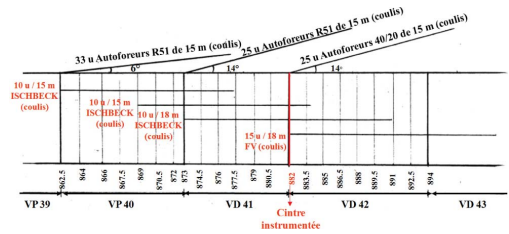


Figure 2.2. Prereinforcements applied at the studied section zone.

2.3 Excavation method

The south Toulon tunnel is excavated on the basis of the so-called “ADECO-RS” method developed by Lunardi (2008). This method is based on the principle that protecting and improving the strength and deformation characteristics of the ground ahead of the tunnel face permits to realize full face excavations of tunnels even under difficult ground conditions. Controlling the deformation response of the ground in the core ahead of the face tunnel is essential to increase tunnel stability and to reduce tunnel deformations and also surface settlements in case of shallow tunnels (Lunardi, 2008).

The reinforcements installed in the ground mass surrounding the monitoring section are (see Fig. 2.2):

- an umbrella composed by 25 autodrilling steel tubes, 14° of inclination, sealed by grout and renewed just after the analyzed section. The umbrella represents in Lunardi’s theory a “protective conservation”: it has to channel the stresses around the advance core in order to maintain the natural soil strength.
- 10 horizontal steel bolts (anchorage > 9 m), sealed by grout and renewed just after the section. They correspond to “reinforcement conservation”: the bolts improve directly the natural strength and deformation characteristics of ground in the core ahead of the tunnel face.

The excavation progresses generally by 1.5 m steps and after each step one HEB 180 steel rib is installed. The tunnel invert, in this zone, was realized with a distance to tunnel face of about 40 m.

3 MEASUREMENT RESULTS

In the following paragraph, the major monitoring results on this section are presented and analysed.

3.1 Inclinerometers

Figure 3.1 shows, in the transverse plane, the lateral displacements of the inclinometer tubes at the most significant moments. The measures were

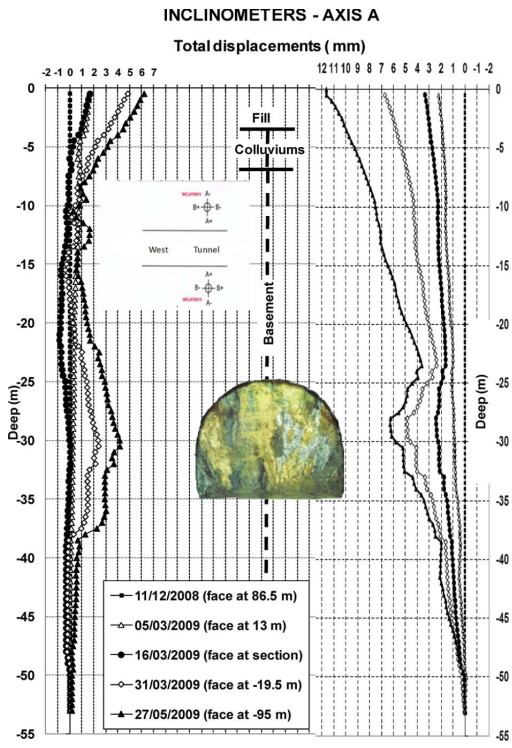


Figure 3.1. Inclinerometers—Axis A.

corrected taking into account the horizontal movements of the surface target prisms recorded by theodolites. One further correction was made after spiral inclinometer surveys.

The analysis of the curves shows two phenomena:

- the first few meters of inclinometers converge towards the tunnel;
- a local convergence (“belly”) is also observed at the tunnel level.

Both phenomena increase until stabilization approximately 80 m after the tunnel face has crossed the section.

Some movements appear 1.5 times the tunnel diameter below the tunnel invert. This confirms the necessity to install the inclinometer base largely below the tunnel in order to ensure an anchored zone and be able to accurately analyse the monitoring data.

The measurements also show a dissymmetry of the ground structure caused by local effects due to soil heterogeneity.

The inclinometers movements parallel to the tunnel axis (Axis B) were analyzed as well. Figure 3.2 shows the South inclinometer movements.

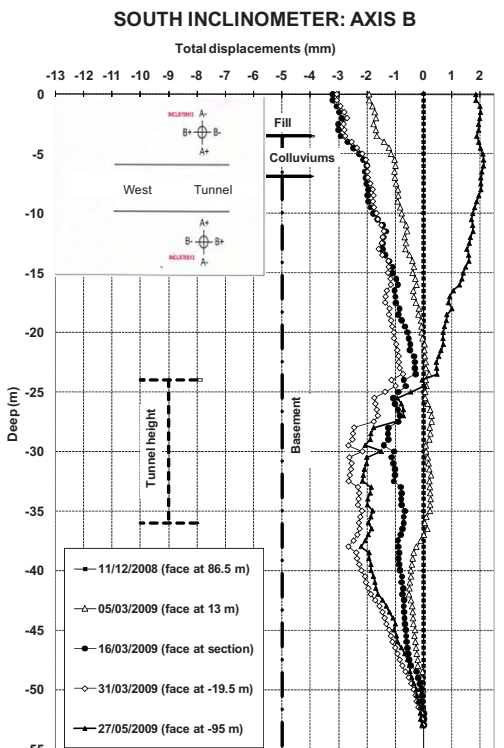


Figure 3.2. South Inclinerometer—Axis B.

The upper 25 m move towards the tunnel when it approaches. This movement is maximum when the tunnel face reaches the instrumented section. Then, the horizontal displacement decrease, go back to their initial values and in a last phase increase in the direction of the tunnel face progression.

At the same time, a local displacement at the tunnel level (“belly”) appears and increases as the tunnel face approaches. This demonstrates that the extrusion movements concern not only the tunnel face but also an area of the ground which is at least 13 m far from the tunnel axis. Contrary to what happens in the first meters, this “belly trend” remains even after the tunnel face has passed the monitoring section. This local displacement is an indicator of the volume loss taking place ahead of the face and which will not be recovered.

The results obtained with the inclinometers are in agreement with those analysed by Serratrice (1999) in the north Toulon tunnel in the so-called “plot Chalucet” transverse section. They clearly show that the deformation field induced by the tunnel excavation process is three-dimensional. This does not result in a transverse 2D displacement field when the excavation is completed.

3.2 Analysis of surface target prisms movements

Automatic stations measured the X, Y, Z movements of the target prisms situated close to the two inclinometers and the extensometer heads. Unfortunately, the target prism next to the North inclinometer was damaged, therefore the measures can not be used.

The horizontal displacements in a direction parallel to the tunnel axis are shown in Figure 3.3, and confirm the inclinometer measurements. When the tunnel face is at approximately 35 m, the target prisms start to move towards the excavation.

As in the inclinometers results along axis B, the targets movements attain their maximum approximately at the tunnel face passage. Then, the target prisms start to move in the opposite direction, first coming back to their initial position and then reaching a final positive value. The stabilization is observed when the tunnel face is 80 m away from the section.

The vertical prisms movements were analyzed as well (Fig.3.4). They confirm the excavation starts to have an influence on settlements 35 m ahead of the tunnel face. When the excavation reaches the section the movements accelerate. Then, the settlements velocity decreases and a final stability appears over 90 m behind the tunnel face. The maximum observed settlement is about 20 mm.

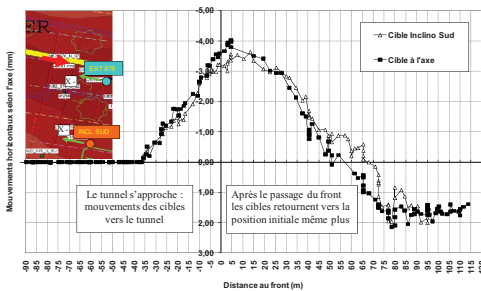


Figure 3.3. Prisms horizontal movements along tunnel axis.

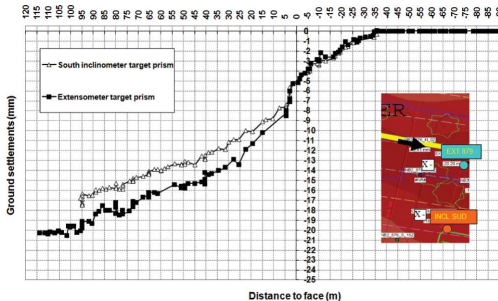


Figure 3.4. Prisms vertical movements.

Some of these results are in accordance with Rankin (1988) who finds that, at a distance to the face equivalent to twice the tunnel cover, the subsidence reaches a value equal to 84% of the expected subsidence. In the studied case, at 60 m far from the face (2 times the overburden), the measured settlement is about 16 mm, 80% of the final settlement (20 mm).

Thanks to the other surface measures close to the section a transverse settlement profile was studied.

With the advance of the tunnel excavation, a three-dimensional settlement trough is developed at the ground surface. On the basis of many field observations, Peck (1969) showed that this shape in a plane transverse to the axis of the tunnel can be represented by a Gaussian normal distribution curve, defined by 2 parameters: S_{max} , the settlement on the tunnel axis and i , the distance of the inflection point to the axis. This assumption was confirmed by the results of numerous in situ measurements conducted by Schmidt (1969), Attewell and Farmer (1974) and from small scale laboratory models carried out by Atkinson and Potts (1977).

A Peck optimization with the method of least squares was made on in situ measures (Fig. 3.5). In order to have more data, the settlement profiles of the sections close to the studied one were considered as well. The measures were normalized on the maximum settlement of each section. In comparison to the classical Gauss formulation, an x_0 parameter was added to represent an horizontal translation of the settlement trough. The formula becomes:

$$S(x) = S_{max} \exp\left(\frac{-(x-x_0)^2}{2i^2}\right) \quad (1)$$

The optimization confirms a translation value of 2.1 m towards the South. This was also found by Serratrice (1999) for the analysis of the transversal settlement profiles of the North Toulon tunnel. It is caused by a dissymmetry of the soil structure.

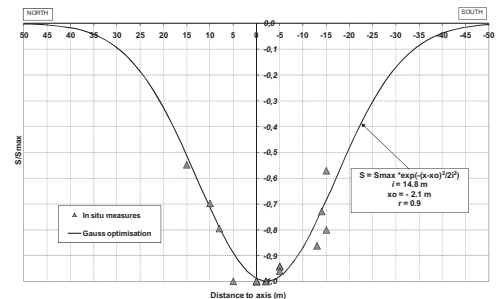


Figure 3.5. Gauss optimization of settlements profile.

The width of the settlement trough is taken equal to 14.8 m. O' Reilly and New (1982) made the hypothesis that this width can be estimated by an empirical parameter K, such as $i = K \cdot Z_0$ (with Z_0 the depth of the tunnel axis) depending on the ground conditions. Values close to the lower limit ($K = 0.2$) are characteristic of loose grounds while values close to the higher limit ($K = 0.7$) can be associated to cohesive grounds (O'Really and New 1982, Yeates 1985).

Based on a large number of observations, Mair and Taylor (1997) concluded that K varies from 0.25 to 0.45 for sands and gravels and is close to 0.5 for short term settlement of clays, whether they are stiff or soft.

With the i value obtained from optimisation, K is, in the case of the monitored section, equal to 0.48.

Bilotta, Russo and Viggiani (2002) have collected approximately 90 cases of green field transverse settlement troughs of urban shallow tunnels. As in this study, they have interpolated with Gaussian curve the measures and, thanks to an optimization with the least squares method, they obtained the i parameters. Then they studied the K variation for all cases (see Fig. 3.6). The calculated arithmetic mean is 0.43 and the mean square deviation is equal to 0.20. Therefore the K obtained with our measures is within the average of their study.

It is possible also to calculate the ground settlement volume (V_s) using the following formula (for $i = 14.8$ m, $S_{max} = 0.020$ m):

$$V_s = i \cdot S_{MAX} \cdot \sqrt{(2 \cdot \pi)} = 0.74 m^3/m \quad (2)$$

The volume loss in comparison to the theoretical excavated volume ($120 m^3$) is $V' = 0.62\%$. This result agrees with the V' values calculated by Bilotta, Russo and Viggiani (2002) on in situ cases.

3.3 Vertical extensometer

The extensometer is composed by 5 anchors at 5 different depths (6, 12, 16, 18 and 19 m from the surface). The displacements between each anchor and the instrument head were recorded with a microm-

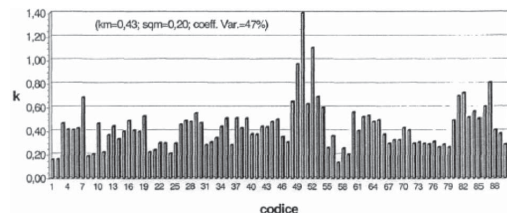


Figure 3.6. Barr chart of k values obtained from studied case - Bilotta, Russo and Viggiani (2002).

eter. The settlements of the prism placed close to the extensometer head were added to obtain the total anchors movements. Due to problems with embedded instruments, only the measures of the two upper anchors are active.

Figure 3.7 shows the settlement of these 2 anchors plotted against the distance between the instrument and the tunnel face. The settlement trend of the two anchors is very similar and indicates that the upper twelve meters of soil above the tunnel crown behave as a rigid block.

3.4 Pressure cells

The pressure cells were placed between the soil and the shotcrete when the tunnel face reached the analysed section. The installation was difficult due to the over-excavations beyond the rib that induces a bad contact between the soil and the instrument. The measures obtained are not very satisfactory due to the installation and to the high sensibility to temperature variation.

3.5 Vibrating strain gauges

Six couples of strain gauges (intrados and extrados) were welded on the rib directly above the analysed section. The strain gauges permit to calculate forces in the rib by measuring the steel deformation.

Just after the gauges installation, measures appear to be extremely sensitive to temperature variation. Then, a direct relation appears between each new step of excavation and stress increasing on the rib. There is a regular increase of the above mentioned stress till the tunnel face is 20 m away from the instrumented section. Afterwards, the measures show a small stress increase and a final stability appears after 100 m. The stabilised measures analysis indicates that the stress decreases from the crown to the tunnel invert.

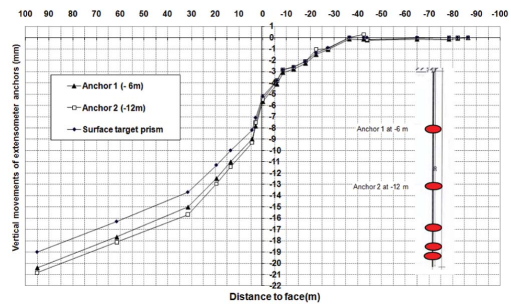


Figure 3.7. Total vertical movements of extensometer anchors.

The final values at the extrados (σ_e) and intrados (σ_i) measured by the gauges are used to calculate the axial force (N) and the bending moment (M) in 5 different positions along the rib (see Fig. 2.1). One of the gauges, placed at the tunnel crown, did not work.

Table 3.1 presents the forces calculated on the steel rib. The average axial force presents its maximum at the tunnel crown and decreases progressively towards side walls. The bending moment is positive and maximum at the tunnel crown. Then, at points 2 and 3 it becomes negative. Finally, the values show a dissymmetry in the steel rib lower parts.

3.6 Convergence and tunnel settlements

In the Toulon tunnel, the convergence in six directions and the settlement of five targets have been regularly measured by traditional topography.

The tunnel deformation was compared with the ground surface settlements in the analysed section. The results show that the underground deformations propagate towards the ground surface approximately with no delay and no damping.

Considering the stabilised final convergence, it is possible to draw the tunnel section deformation (see Fig. 3.8). This represents a qualitative inter-

Table 3.1. Axial forces and bending moments on the rib.

	σ_e (MPa)	σ_i (MPa)	N (MN)	M (KN·m)
1	175.9	142.6	0.96	12.37
2	76.4	106	0.60	-6.32
3	95.1	107.4	0.66	-2.61
4	42.2	42.5	0.28	-0.07
5	60.5	36.1	0.32	5.18

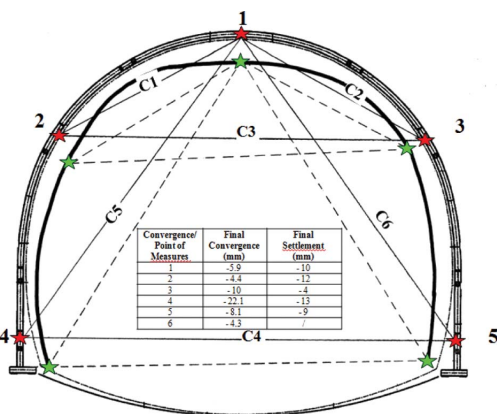


Figure 3.8. Rib deformation, qualitative interpretation.

pretation based on the previous calculated bending moment and the following hypothesis:

- the horizontal movement of tunnel crown target is equal to zero;
- the convergences are symmetrical.

3.7 Radial extensometers

Four radial extensometers were installed from the tunnel (see Fig. 2.1). Their installation was very difficult because after each drilling the hole was closing and it was not possible to easily set the instrument inside.

As an example, Figure 3.9 shows in the case of extensometer #4 the variations of the distance between the anchors and the extensometer heads (see Fig. 2.1) in relation with time and the underground activities. Negative distance corresponds to an extension between the anchor and the extensometer head. The anchors at 7.5 m and 4.5 m seem to belong to a homogeneous ground mass. On the contrary, the anchor at 2 m is in a more deformable part. It is evident that the excavation progress, i.e. VD 42, causes movement acceleration. This phenomenon ends once the tunnel face arrives 60 m away from the section and the radial displacements stabilises.

3.8 Correlation between the different measures

The data recorded by different instruments are compared (see Fig. 3.10).

The Northern and Southern vertical inclinometers both cross the radial extensometers n°4 and n°5 respectively in the vicinity of the anchor located 7.5 m from the tunnel. Thanks to this, the radial movements of the two tunnel side walls can be calculated.

In fact, the radial movement (U_r) is equal to the sum of the extension between the extensometer head and the anchor at 7.5 m and the horizontal

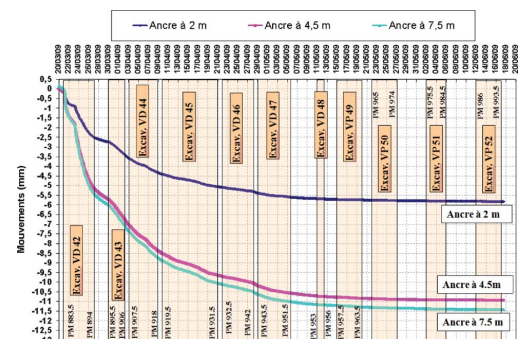


Figure 3.9. Anchors movements of extensometer # 4.

displacement of the same anchor which was measured by the inclinometer, since the tunnel face reaches the instrumented section.

The sum of the two abutment movements (23.1 mm) should then be equal to the convergence C4 measured by topography (22 mm). The comparison between the two above mentioned methods is very satisfactory and such results confirm the good accuracy of measurements.

4 2D NUMERICAL SIMULATION

All these measurements have permitted to create a significant database. The objective of the study is to carry out a back analysis on these data with numerical calculations. The main goal is to improve the settlements prediction, based on numerical approach, for the tunnels excavated with the pre-reinforcement techniques.

The first simulation was carried out with the finite element code PLAXIS 2D. The model represents the geometry of the section previously described. A linear elastic perfectly-plastic constitutive model with a Mohr-Coulomb failure criterion is considered for the soil layers. The steps of the calculation are the following:

1. Ground stress initialization (drained conditions).
2. Tunnel excavation with a stress release coefficient λ_1 .
3. Application of reinforcement on side walls and key tunnel with a stress release coefficient λ_2 .
4. Setting up of the tunnel invert and full stress release ($\lambda = 1$).

The comparison between the numerical outcomes and in situ measurements shows that it is not possible to represent the correct trend of inclinometer horizontal movements using a homogeneous Young's modulus (E) for the Basement layer. In order to solve this problem the Basement is divided in three layers with different moduli, that increase with depth (Fig 4.1).

This solution permitted to obtain numerical results that fit well the in situ measures. Figure 4.2 and Figure 4.3 show the settlement profile in the transverse section and the horizontal movements of the lateral inclinometer. These numerical results are obtained with stress release coefficients λ_1 and λ_2 respectively equal to 0.4 and 0.5.

This first simulation highlights that the used simple constitutive model is not able to represent the real soil behavior. It is necessary to adopt a more complex constitutive model that is able to take into account the non-linearity of soil behavior before

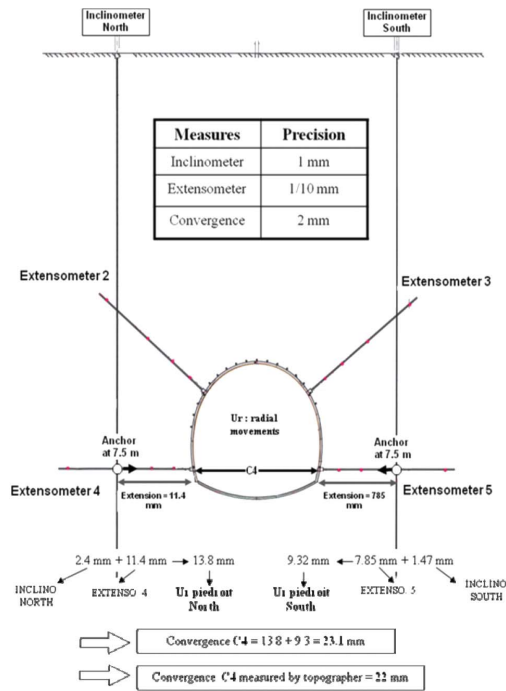


Figure 3.10. Correlation between the different measures method.

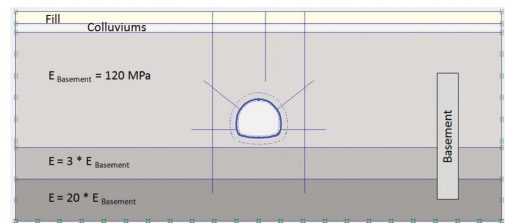


Figure 4.1. 2D numerical model (PLAXIS 2D).

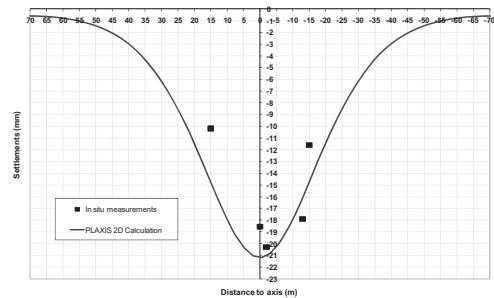


Figure 4.2. Settlement profile in the transverse section - comparison between 2D numerical simulation and in situ measures.

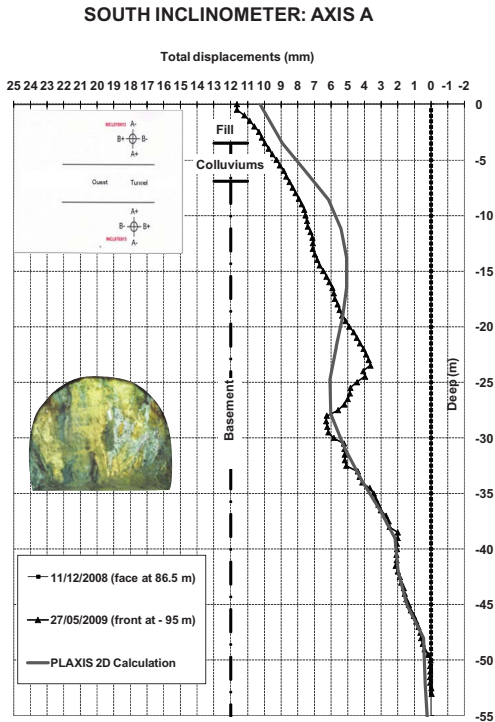


Figure 4.3. Inclinometer horizontal movements - comparison between 2D numerical simulation and in situ measures.

failure. This constitutive model must simulate unloading stress paths using a modulus that is different from the loading one.

5 CONCLUSION

The monitoring section, installed during the construction of the south Toulon tunnel, has permitted to analyse the evolution of soil deformation with the excavation progress. The comparison between the measures realized from the ground surface with those carried out from the tunnel proves the global coherence and accuracy of results.

The experimental data show that the excavation has an influence of 3 times the tunnel diameter ahead of the tunnel face. Then, a global stabilisation is reached about 90 m behind the tunnel face.

The analysis of inclinometers results highlights that the deformation field induced by the tunnel excavation process is fully three-dimensional.

The extensometer outcomes display that the upper twelve meters of soil above the tunnel crown behave as a rigid block.

The instruments placed close to the rib show a direct relation between the excavation progress and the increasing stress on the reinforcement.

Finally, this monitoring section has permitted to create a database of accurate measures that allow validating numerical simulations. Through 2D and 3D numerical approaches, based on the monitoring section, the effects of the pre-reinforcement techniques on the stress release will be studied.

REFERENCES

- Atkinson, J.H. & Potts D.M. 1977. Subsidence above Shallow Tunnels. *Journal of Geotechnical Engineering*, ASCE, Vol. 103, No.4: 307–325.
- Attewell, P.B & Farmer I.W. 1974. Ground deformation resulting from shield tunnelling in London clay. *Canadian Geotechnical Journal*, Vol. 11: 380–396.
- Attewell, P.B., Yeats, J. & Selby, A.R. 1986. Soil movements induced by tunnelling and their effects on pipelines and structures. Glasgow: Blackie.
- Bilotta, E., Russo, G., & Viggiani, C. 2002. Cedimenti indotti da gallerie superficiali in ambiente urbano. XXI Convegno Nazionale di Geotecnica: 487–494. L'Aquila.
- Janin, J.P., Dias, D., Emeriault, F., Kastner, R., Lebissonnais, H. & Guilloux, A. 2011. Settlement monitoring and tunneling process adaptation—case of South Toulon Tunnel. *The seventh International Symposium on "Geotechnical Aspects of Underground Construction in Soft Ground"*, *tc28 Rome*. Rome.
- Mair, R.J., Taylor, R.N., 1997. Bored tunneling in the urban environment. *Proc. Conf. on Soil Mechanics and Foundation Engineering*, Theme lecture. Hamburg.
- Lunardi, P. 2008. Design and construction of tunnels—Analysis of controlled deformation in rocks and soils (ADECO-RS): 577. Springer—Verlag Berlin Heidelberg.
- O'Reilly, M.E., New, B. 1991, Tunnelling induced ground movements predicting their magnitude and effects. *4th International Conference on Ground Movements and Structure*. Cardiff.
- Peck, R.B. 1969. Deep excavation and tunnelling in soft ground 7th ICSMFE. *State of the art Volume*: 225–290. Mexico City.
- Rankin, W.J. 1988. Ground movements resulting from urban tunnelling: prediction and effects. *Engineering Geology of Underground Movements*: 79–92. London: F.G. Bell et al.
- Serratrice, J.F. 1999. Suivi du plot Chalucet, application à la prevision des tassements de surface pendant le creusement du tunnel de Toulon, *Journée de Mécanique des Sols et des Roches d'Aix en Provence*: 31.
- Schmidt, B. 1969. Settlements and ground movements associated with tunneling in soil. *PhD thesis*. University of Illinois.